International Journal of Microwave and Wireless Technologies

cambridge.org/mrf

Research Paper

Cite this article: Mandal S, Karmakar A, Singh H, Mandal SK, Mahapatra R, Mal AK (2020). A miniaturized CPW-fed on-chip UWB monopole antenna with band-notch characteristics. *International Journal of Microwave and Wireless Technologies* **12**, 95–102. https://doi.org/10.1017/S1759078719000941

Received: 18 July 2018
Revised: 6 June 2019
Accepted: 6 June 2019
First published online: 3 July 2019

Key words:
Bandwidth ratio; CPW; fractional bandwidth; on-chip antenna; VSWR; ultra-wideband (UWB)

Author for correspondence:
S. Mandal, E-mail: sanjuktamandal2@gmail.com

A miniaturized CPW-fed on-chip UWB monopole antenna with band-notch characteristics

S. Mandal[1], A. Karmakar[2], H. Singh[1], S. K. Mandal[1], R. Mahapatra[1] and A. K. Mal[1]

[1]Department of Electronics and Communication Engineering, NIT Durgapur, West Bengal 713209, India and [2]Department of Space, Semi-Conductor Laboratory, Punjab 160071, India

Abstract

This paper presents the design and analysis of a miniaturized, coplanar waveguide-fed ultra-wideband monopole on-chip antenna with band-notch characteristics. By incorporating a "U"-shaped slot in the feedline, a band-notch is realized in the frequency range of 7.9–8.4 GHz to avoid interference from the X-band uplink satellite communication system. The proposed antenna achieved good voltage standing wave ratio (VSWR) characteristics with VSWR value <2 for the frequency range of 2.5–20.1 GHz excluding the band-notched frequencies. The fractional bandwidth and bandwidth ratio are obtained as 156% and 8.04:1, respectively. Dominant factors that affect the center frequency and bandwidth of the notched band are thoroughly investigated. This paper addresses both frequency as well as time domain behavior of the proposed structure. Standard 675 μm thick, high resistive silicon substrate ($\rho \geq 8$ kΩ-cm, $\epsilon_r = 11.8$, and $\tan\delta = 0.01$) is used to design the proposed compact antenna structure with a layout area of 8.5×11.5 mm^2. Fabrication process steps along with simulated and measured data are presented here. A close analogy between simulated and measured data is observed.

Introduction

U.S.-based independent agency, Federal Communication Commission (FCC) has approved the usage of ultra-wideband (UWB) (3.1–10.6 GHz) as an unlicensed spectrum in 2002 [1]. UWB technology offers high performance and high security in both indoor and outdoor wireless communication systems. Currently, UWB technology is being used in various applications ranging from radar to high data-rate personal area network. Furthermore, it can also be used in both commercial and military applications. However, the wide frequency range of UWB may cause interference with the already existing licensed spectra such as WiMAX band (3.3–3.7 GHz), WLAN band (5.15–5.85 GHz), ITU-8 band (7.9–8.8 GHz), etc. Rejection capability of a UWB antenna is required to avoid interference from the abovementioned licensed frequency bands. In this regard, during the last few decades, antenna researchers have reported several methods for designing a compact UWB antenna with integrated band-notch filtering capability [2–16].

Single-notch filtering functionality is realized by introducing different slot structures either in ground plane or in radiating patch. For example, an inverted L-shaped slot is included in the ground plane [2], while U-shaped [3], W-shaped [4], hat-shaped [5], and cup-shaped [6] slots are incorporated in the radiating patch. Antennas with dual- [7–9], triple- [10, 11], and quad- [12, 13] notched characteristics by using different combinations of various slots have also been reported. Although incorporation of slot structures is a simple and popular approach, other options such as introducing parasitic strips above the ground plane [14], use of split-ring resonators [15], and Hilbert curves [16] are also found to be very effective at notch out the desired frequency band.

To establish a high data-rate communication link, RF engineers are still trying to stretch the impedance bandwidth beyond the specified UWB range. Toward this, different techniques such as inserting an inverted T-shaped notch in the ground plane [17], by incorporating a pair of L-shaped conductor-backed planes, and a pair of modified L-shaped slots on the radiating patch [18], by using fractal structures such as Penta-Gasket-Koch [19] and Sierpinski Carpet geometry [20], have been reported in various papers.

All of the abovementioned antennas have been designed on low-loss printed-circuit boards such as FR4-epoxy and Rogers RT/duroid 5880, and they are termed off-chip antennas. However, to meet the requirement of obtaining a compact system, research on designing antennas on a silicon substrate (generally termed on-chip antennas) is going to be the future trend. Such on-chip antennas can be easily integrated with other necessary digital and analog modules required for making a compact system-on-chip (SoC) [21]. Though

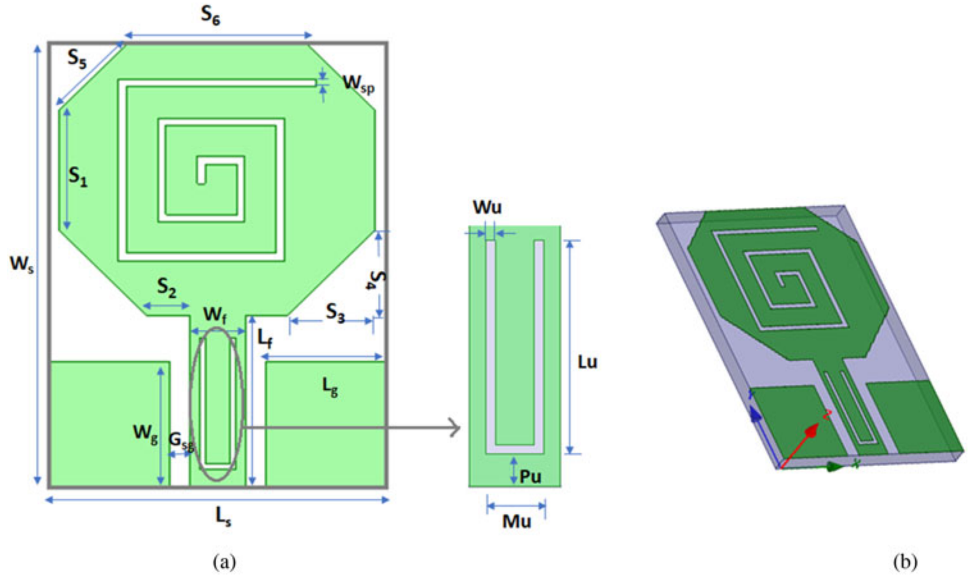

Fig. 1. Design layout of the proposed UWB antenna: (a) top view and (b) 3D view.

Table 1. Optimized parameter values of the proposed antenna (unit: mm)

Parameter	L_s	W_s	L_g	W_g	L_f	W_f	M_u
Value	8.5	11.5	3.04	3.3	4.5	1.4	0.9
Parameter	L_u	W_u	P_u	W_{sp}	G_{sg}	S_1	S_2
Value	3.4	0.15	0.5	0.2	0.51	3.1	1.1
Parameter	S_3	S_4	S_5	S_6			
Value	2.2	2.2	2.4	4.6			

most of the reported on-chip antennas are for 60 GHz communication [22–24], research on UWB antennas using silicon as a substrate is still rudimentary. In 2007, Yan *et al.* proposed an on-chip antenna for IEEE 802.11a and UWB applications [25]. Jiang *et al.* reported a novel complementary metal–oxide semiconductor (CMOS) process-based on-chip antenna that can be used in UWB wireless inter-/intra-connects or a wireless chip area network [26]. Kimoto *et al.* demonstrated UWB signal transmission among silicon integrated circuits (ICs) using linear dipole antennas [27]. UWB antenna on a silicon substrate with notched characteristics was first reported in [28]. Another coplanar waveguide (CPW)-fed UWB antenna on silicon substrate with dual band-notch characteristics was demonstrated in [29].

In this paper, the proposed work mainly highlights two crucial aspects. The first one is to design a compact monopole antenna on silicon substrate with operating bandwidth extended beyond the specified UWB range. The next one is to incorporate band-notch filtering capability to mitigate interference from the 7.9–8.4 GHz band assigned by International Telecommunications Union (ITU) for X-band uplink satellite communication systems. This proposed antenna is compact as compared with the reported antenna structures in [2–20, 28, 29]. It also provides large impedance bandwidth as compared with the related antennas published in [2–25, 28, 29]. This compact antenna with higher bandwidth is suitable to meet the requirement for its applicability in the present short-range, high data-rate communication systems. Also, the proposed antenna designed on the Si substrate has the potential to be integrated with other modules on the same substrate using single process technology to make an application-specific, truly efficient, compact SoC at a reduced cost.

The rest of the paper is organized as follows. Detailed description of the antenna design steps is presented in the "Antenna design and analysis" section. The "Fabrication process" section gives the briefing of the fabrication process steps. Different performance parameters of the antenna in both frequency and time domain are demonstrated in the "Results and discussion" section. Finally, some concluding remarks are given in the "Conclusion" section.

Antenna design and analysis

The top view and 3D view of the proposed antenna structure are shown in Figs 1(a) and 1(b), respectively. It consists of an irregular octagonal patch with a spiral-shaped slot within it. Table 1 shows the optimized values of the corresponding design parameter. CPW feeding is preferred here over the microstrip line to avoid any kind of interference of the EM field with another IC component. This interference generally occurs when a ground plane is placed below the substrate [21]. The feedline with the G/W/G configuration of 0.51/1.4/0.51 (mm) is used to materialize 50 Ω impedance.

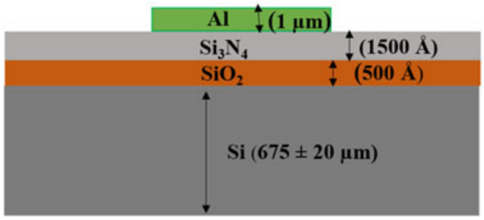

Fig. 2. Layered view of the antenna.

An FEM-based EM simulator HFSS v17 is used to analyze the 3D antenna structure. The standard CMOS process with only one level of mask (metal patterning) has been used to realize the structure. Layered view of the antenna is shown in Fig. 2.

Figure 3 depicts the stepwise modifications as required to realize the proposed structure and the corresponding frequency response characteristics of the respective design steps are shown in Fig. 4. First, a CPW-fed rectangular monopole antenna having a layout area of 8.5×11.5 mm^2 was taken as a reference antenna (Fig. 3(a)) that operates in the frequency range of 2.43–12.8 GHz. In the second step, a rectangular spiral slot is included within the patch (Fig. 3(b)). Incorporation of the slot within the patch excites higher order modes which overlap with the fundamental mode of the reference patch antenna. This excitation of the higher order modes overlapping with the original bandwidth results in the enhancement of the overall operating bandwidth of the modified design by 1 GHz (operating band 2.45–13.82 GHz). To increase the bandwidth further, four triangular portions are etched out from the four corners (Fig. 3(c)). This corner truncation technique provides increased bandwidth by creating multiple reflections of the surface current from the edged corners. As a consequence, the upper cut-off frequency is shifted to the right-hand side to a great extent. In this step, the bandwidth is enhanced by 6.68 GHz with operating the frequency range of 2.63–20.68 GHz. Finally, in the fourth step, the "U"-shaped slot is incorporated into the feedline (Fig. 3(d)) to achieve band-notch characteristics. The total length of this slot is approximately equals to the half of the guided wavelength ($\lambda_g/2$) corresponding to the desired center frequency $f_c = 8.2$ GHz which is the mid-frequency of the targeted notched band 7.9–8.4 GHz. This "U"-shaped slot in the feedline acts like a band reject filter by confining most of the surface current within it and allowing a minimal amount of current to flow to the radiating patch. As a result, the antenna remains irresponsive within the frequency range of the targeted notched band.

The "U"-shaped slot has a very simple geometry along with four parameters such as arm length (L_u), width (W_u), separation between two arms of the slot (M_u), and distance from the bottom (P_u). After a thorough investigation using parametric analysis, it is found that L_u and P_u are the dominant factors which affect the center frequency (f_c) and bandwidth of the notched band respectively. The effect of L_u on f_c is shown in Fig. 5. It is observed that, with the increment of L_u from 2.5 to 3.8 mm, f_c decreases from 11.08 to 7.27 GHz.

Table 2 shows different values of L_u and their corresponding total slot length values L_t and as well as simulated f_c values. From the geometry of the slot (Fig. 1(a)), L_t can be obtained using the following equation:

$$L_t = 2L_u + M_u - 2W_u \tag{1}$$

Now, for each value of f_c, guided wavelength λ_g can be calculated using the following formula:

$$\lambda_g = \frac{\lambda_0}{\sqrt{\varepsilon_{eff}}} = \frac{c}{f_c\sqrt{\varepsilon_{eff}}} \tag{2}$$

where c is the speed of light in free space and ϵ_{eff} is the effective permittivity of the material. For the substrate having a low thickness, ϵ_{eff} can be calculated using the following approximate formula [30, 31]:

$$\varepsilon_{eff} \approx \frac{\varepsilon_r + 1}{2} \tag{3}$$

where ϵ_r is the relative permittivity of the material.

It is clear from Table 2 that the total slot length should be approximately equal to half of the guided wavelength to obtain the desired center frequency of the notched band. In the proposed antenna, the desired notched band is 7.9–8.4 GHz with the center frequency of 8.2 GHz. Corresponding to the desired center frequency, the optimum value of L_u is obtained as 3.4 mm.

Now keeping L_u fixed at its optimum value, bandwidth of the notched band is adjusted by changing P_u. Figure 6 shows the effect of P_u on the bandwidth of the notched band. It is observed that the increment of P_u results in decrement of bandwidth. When P_u increases from 0.5 to 0.8 mm, bandwidth decreases from 830 to 720 MHz. It can also be noted that changing P_u from its optimum value of 0.5 mm results in decrement of the peak value of rejection ratio. Table 3 lists the obtained notched bandwidth value corresponding to P_u.

Fabrication process

High resistive, FZ processed silicon wafer ($\rho \geq 8$ kΩ-cm, tan $\delta = 0.01$, and $\epsilon_r = 11.8$) with the thickness of 675 ± 20 µm has been chosen as the antenna substrate. The surface of the wafer is oxidized to form a layer of SiO_2 having a thickness of 0.05 µm that acts as an insulating membrane. As SiO_2 generates some compressive stress on the wafer, another 0.15 µm thin layer of silicon nitride (Si_3N_4) is deposited above SiO_2 to counterbalance that effect. These two layers are used as a buffer layer over the silicon substrate. On the top, 1 µm thick aluminum (Al) layer is deposited by DC magnetron sputtering followed by dry etching of the metal using the mask.

Results and discussion

Characteristics in the frequency domain

This section demonstrates different performance parameters of the proposed structure. Along with the inset image of the fabricated prototype, the measured and simulated resonance characteristics of the proposed antenna are shown in Fig. 7. The graph reveals UWB behavior of the proposed antenna having bandwidth extended up to 20.1 GHz from 2.5 GHz along with band rejection capability ranging from 7.8 to 8.7 GHz. The measurement has been carried out using a R&S®ZVA-40. A good agreement between simulated and measured data is obtained up to 17 GHz. The deviation beyond 17 GHz may be due to the inaccuracies that arise at the time of conductive epoxy spreading at the feed point of the antenna. As this step is performed manually, it often results in asymmetrical spreading of the conductive epoxy.

https://doi.org/10.1017/S1759078719000941 Published online by Cambridge University Press

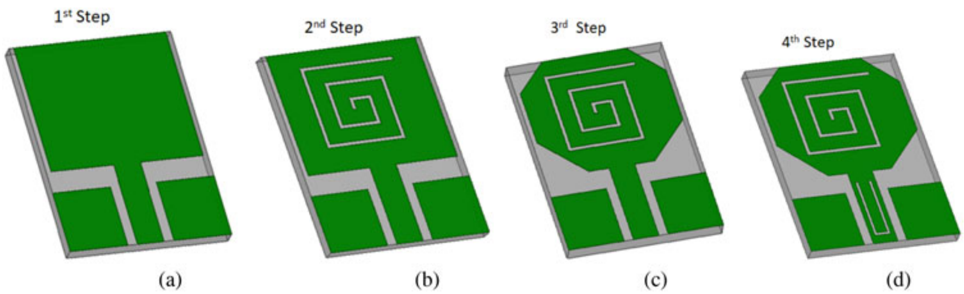

Fig. 3. Design steps of the proposed antenna: (a) reference antenna, (b) inclusion of spiral slot on patch, (c) etching out from the four corners, and (d) inclusion of "U"-shaped slot in the feedline.

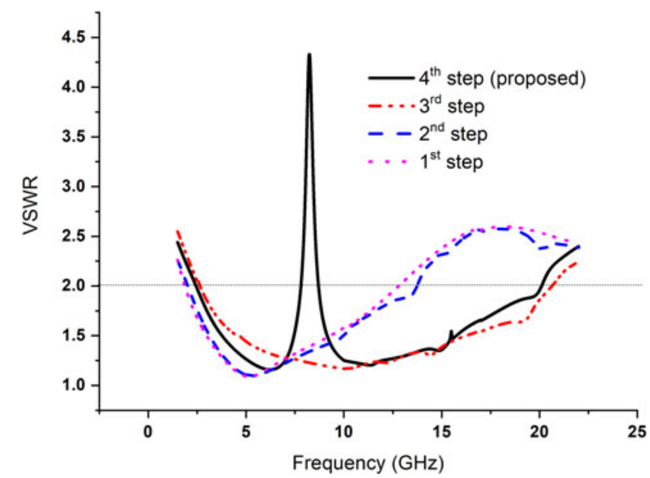

Fig. 4. VSWR characteristics comparison of different design modification steps shown in Figs 3(a)–3(d).

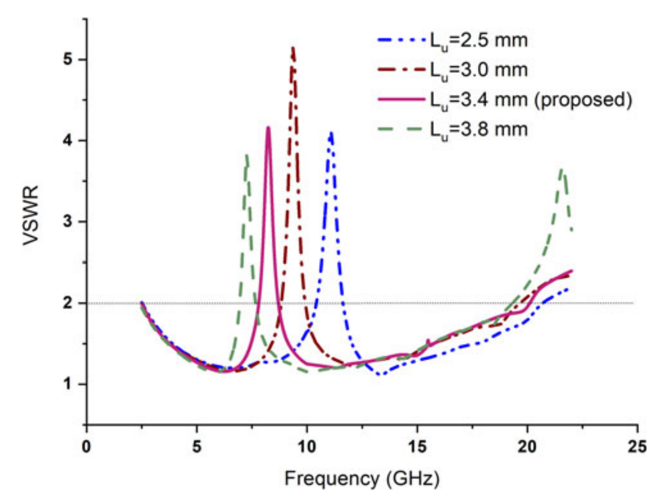

Fig. 5. Effect of L_u on f_c of the notched band for the optimum feedline slot parameters such as $M_u = 0.9$ mm, $W_u = 0.15$ mm, and $P_u = 0.5$ mm.

Table 2. List of the center frequency (f_c) of the notched band for different values of L_u

L_u (mm)	L_t (mm)	f_c (GHz)	$\lambda_g/2$ (mm)
2.5	5.6	11.08	5.35
3	6.6	9.38	6.32
3.4	7.4	8.24	7.2
3.8	8.2	7.27	8.16

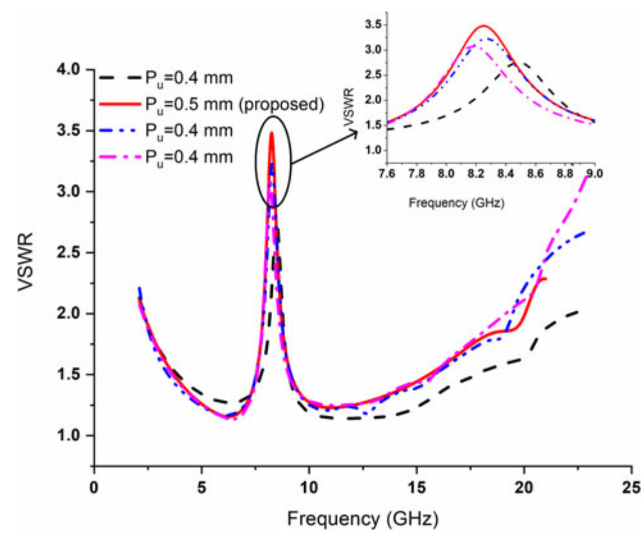

Fig. 6. Effect of P_u on the notched bandwidth with optimum design parameters of the feedline slot such as $L_u = 3.4$ mm, $M_u = 0.9$ mm, and $W_u = 0.15$ mm.

Table 3. Effect of P_u on the bandwidth of the notched band

Parameter (P_u) (mm)	Frequency range (GHz)	Bandwidth (MHz)
0.5	7.86–8.69	830
0.6	7.88–8.69	810
0.8	7.85–8.57	720

It may also cause changes in the pitch size (separation between signal and ground plane) of the actual CPW line. It further degrades the characteristic impedance of the transmission line, which may be responsible for impedance mismatching at any arbitrary frequency. A standard dicing tool with a diamond cutter is used for dicing purpose, and conductive epoxy (H70E) is used as an adhesive material for integrating the RF connector with the antenna.

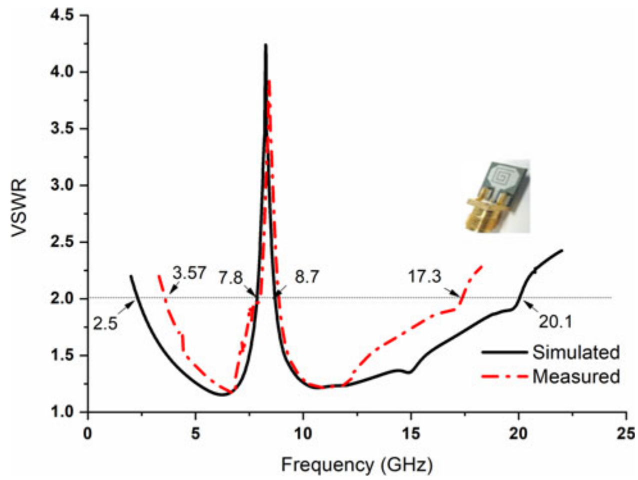

Fig. 7. Comparison of simulated and measured VSWR characteristics.

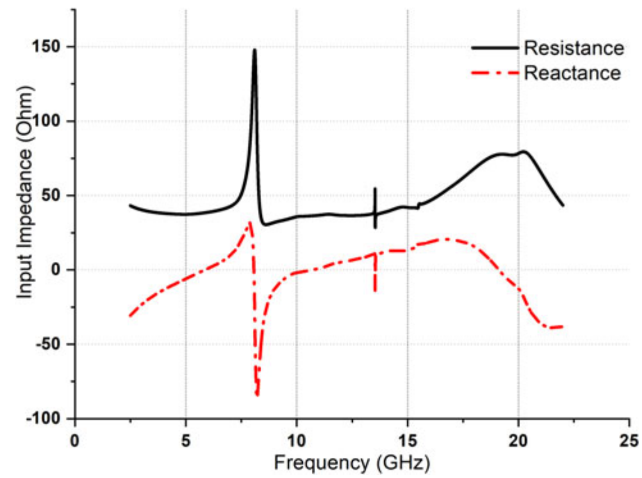

Fig. 9. Variation of real and imaginary parts of the input impedance with frequency.

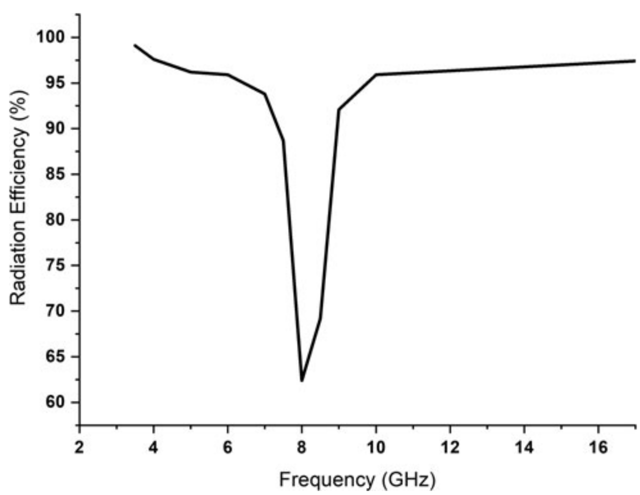

Fig. 8. Plot of radiation efficiency of the proposed antenna with frequency.

Variation of radiation efficiency with respect to frequency is shown in Fig. 8. It is observed that the radiation efficiency lies in the range of 96 ± 1% over the entire band except at the notched band. It sharply decreases to 62% at f_c of the notched band indicating good band-notched characteristic of the proposed antenna.

Figure 9 shows the input impedance variation with frequency. It is seen that the real and imaginary parts of the input impedance oscillate around 50 and 0 Ω, respectively, over the entire operating bandwidth except in the notched region. At the center frequency of the notched band, i.e. 8.2 GHz, the real part of the input impedance reaches 148 Ω, and the imaginary part exhibits parallel resonance characteristics at that frequency.

Figure 10 depicts surface current distributions at 8.2 and 12 GHz. At 8.2 GHz, the current is only concentrated within the "U"-shaped slot in the feedline. The current doesn't reach the radiating patch at all. Therefore, the antenna remains irresponsive at that frequency. At 12 GHz, lying outside the notched band, the current distribution is more at the lower edge of the radiating patch and around the rectangular spiral slot.

Figure 11 depicts the simulated far-field radiation pattern of the proposed antenna in the *XZ* (*H*-plane) and *YZ* planes (*E*-plane) at 8.24, 10, and 16 GHz. The plot indicates that the antenna exhibits an omnidirectional pattern in the *H*-plane and in the *E*-plane, it looks like conventional monopole like pattern. In Fig. 11, it is also observed that there is good isolation between co- and cross-polar levels throughout the entire operating band.

Characteristics in the time domain

The essential parameters of UWB antenna in the time domain are the transfer coefficient $|S_{21}|$ and group delay (τ_g). The group delay can be expressed using the following equation:

$$\tau_g = -\frac{\partial\varphi}{2\pi\partial f} \quad (4)$$

where φ is the phase of the antenna in the far field region and f is the frequency.

Two identical antennas must have to be placed in their far-field region to calculate these two parameters. In this regard, they are positioned here 50 mm apart from each other in both side by side and face to face configurations. Simulated $|S_{21}|$ and group delay are depicted in Fig. 12 and Fig. 13, respectively. It is observed in Fig. 13 that the group delay is almost constant (variation is <1 and 0.5 ns for the side by side and face to face arrangements, respectively) over the entire operating bandwidth except in the notched region. Constant group delay indicates linear variation of the phase with frequency. This criterion, i.e. linear variation of phase with frequency offers distortion-less transmission of pulses by the antenna, and that is the most attractive feature of the proposed UWB antenna.

Conclusion

This paper has demonstrated the detailed design and development of a compact on-chip monopole antenna having fractional bandwidth of 156% which covers UWB (3.1–10.6 GHz), K_u band (12–18 GHz), and some portion of K band (18–26.5 GHz). This antenna has an integrated band-notch filtering capability to avoid interference with the 7.9–8.4 GHz band which is assigned for X-band uplink satellite communication systems. Compact

https://doi.org/10.1017/S1759078719000941 Published online by Cambridge University Press

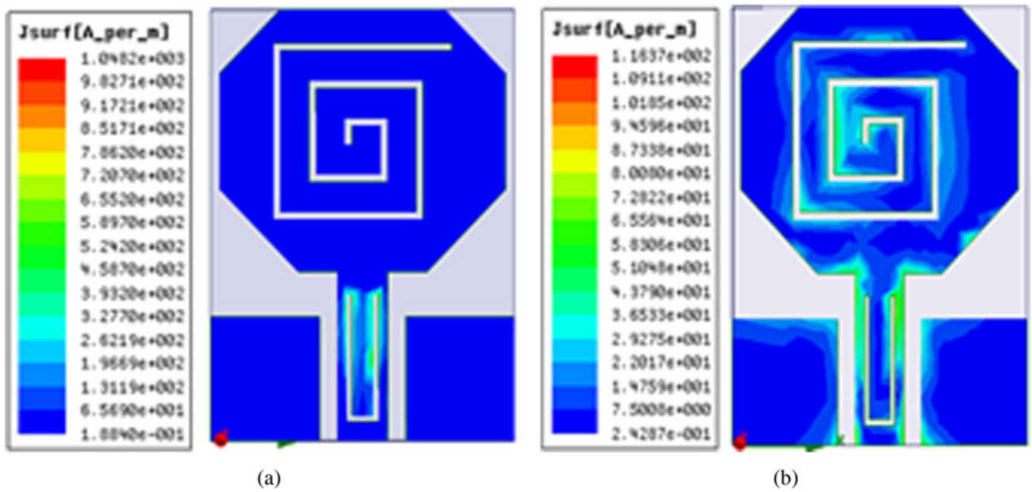

Fig. 10. Current distribution of the designed antenna at center frequency of the notched band and outside the notched band frequency: (a) at $f = f_c = 8.2$ GHz and (b) at $f = 12$ GHz $> f_c$.

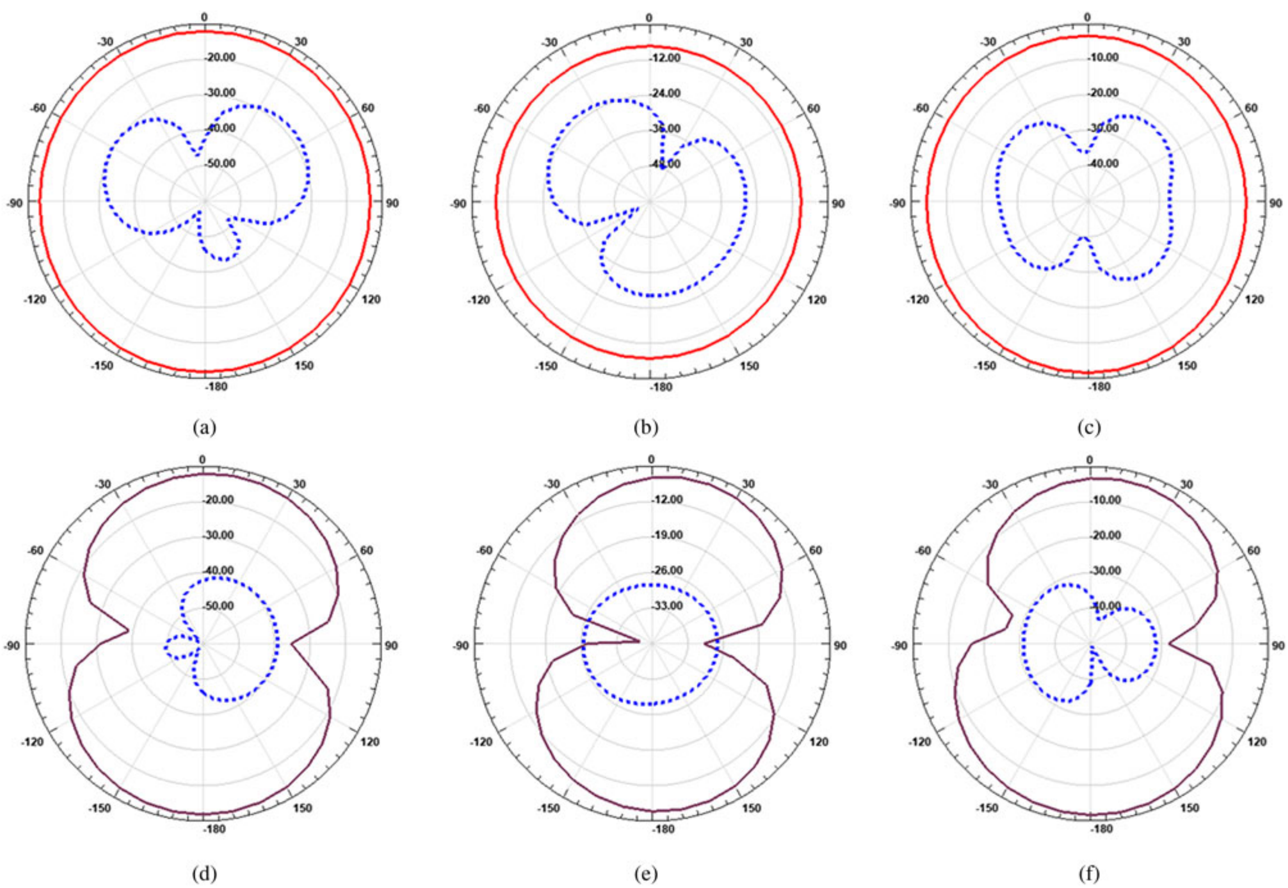

Fig. 11. Simulated *H*-plane and *E*-plane radiation patterns at different frequencies. For *H*-plane at (a) 8.24 GHz, (b) 10 GHz, and (c) 16 GHz; and for *E*-plane at (d) 8.24 GHz, (e) 10 GHz, and (f) 16 GHz.

design (8.5×11.5 mm^2) is the main attractive feature of this research work. The proposed antenna can be used for short-range, high-speed communication. The fabrication process is simple and compatible with the standard CMOS process. Implementation of the antenna on silicon makes it a suitable candidate for future SoC application.

Author ORCIDs. S. Mandal, 0000-0003-3215-2538.

https://doi.org/10.1017/S1759078719000941 Published online by Cambridge University Press

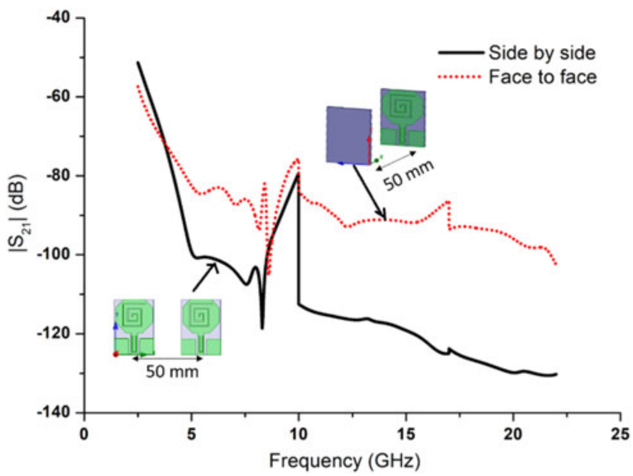

Fig. 12. $|S_{21}|$ characteristics of the proposed antenna for side by side and face to face arrangements.

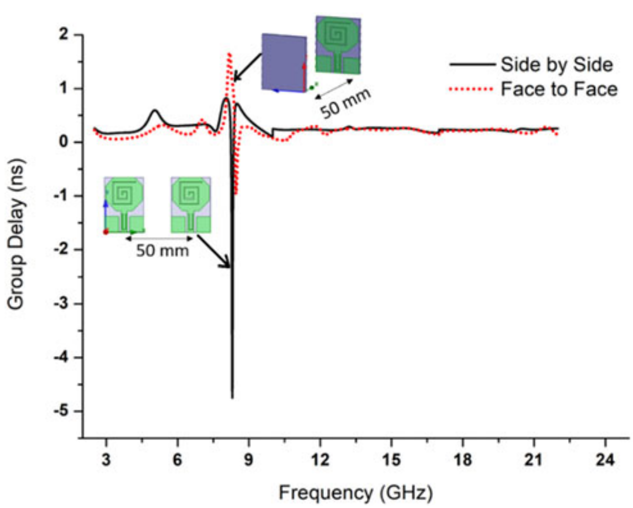

Fig. 13. Group delay variation of the proposed antenna for side by side and face to face arrangements.

Acknowledgement. The authors gracefully acknowledge financial support provided by Visvesvaraya Ph.D. scheme, Ministry of Communications and Information Technology, Govt. of India, Grant No. Ph.D.-MLA/4(29)/2015-16/01 and Special Manpower Development Programme for Chips-to-System Design (SMDP-C2SD) under Govt. of India, Grant No. 9(1)/2014-MDD (Vol III). The authors are also thankful to Semi-Conductor Laboratory (SCL), Chandigarh for providing fabrication and measurement facility.

References

1. **FCC Report and Order of Part 12 Acceptance of Ultra-Wideband (UWB) Systems from 3.1–10.6 GHz. FCC, Washington, D.C., 2002.**
2. **Pancera E, Modotto D, Locatelli A, Pigozzo FM and Angelis CD** (2007) Novel Design of UWB Antenna with Band-Notch Capability. European Conference on Wireless Technologies, Munich, Germany.
3. **Cho YJ, Kim KH, Choi DH, Lee SS and Park S** (2006) A miniature UWB planar monopole antenna with 5-GHz band-rejection filter and the time-domain characteristics. *IEEE Transactions on Antennas and Propagation* **54**, 1453–1460.
4. **Chattha HT, Ishfaq MK, Saleem Y, Huang Y and Boyes SJ** (2012) Band-notched ultrawide band planar inverted-F antenna. *International Journal of Antennas and Propagation* **2012**, 1–6.
5. **Lee HK, Park JK and Lee JN** (2005) Design of a planar half-circle-shaped UWB notch antenna. *Microwave and Optical Technology Letters* **47**, 9–11.
6. **Lee JN and Park JK** (2005) Impedance characteristics of trapezoidal ultra-wideband antennas with a notch Function. *Microwave and Optical Technology Letters* **46**, 503–506.
7. **Modirkhazeni A, Rezaei P and Lafmajani IA** (2015) Compact UWB antennas with inverted E- and F-shaped slots for bandnotch characteristics. *Progress in Electromagnetics Research Letters* **56**, 107–113.
8. **Karmakar A, Verma S, Pal M and Ghatak R** (2012) An ultrawideband monopole antenna with multiple fractal slots with dual band rejection characteristic. *Progress in Electromagnetics Research C* **31**, 185–197.
9. **Biswas B, Ghatak R, Karmakar A and Poddar DR** (2014) Dual band notched UWB monopole antenna using embedded omega slot and fractal shaped ground plane. *Progress in Electromagnetics Research C* **53**, 177–186.
10. **Lin CC, Jin P and Ziolkowski RW** (2012) Single, dual and tri-band-notched ultrawideband (UWB) antennas using capacitively loaded loop (CLL) resonators. *IEEE Transactions on Antennas and Propagation* **60**, 102–109.
11. **Cai ZH, Yang C and Cai LY** (2014) Wideband monopole antenna with three band-notched characteristics. *IEEE Antennas and Wireless Propagation Letters* **13**, 607–610.
12. **Mewara HS, Mahendra DJ, Sharma M and Deegwal JK** (2018) A printed monopole ellipzoidal UWB antenna with four band rejection characteristics. *AEU-International Journal of Electronics and Communications* **83**, 222–232.
13. **Wu Z-H, Wei F, Shi X-W and Li W-T** (2013) A compact quad band-notched UWB monopole antenna loaded one lateral L-shaped slot. *Progress in Electromagnetics Research* **139**, 303–315.
14. **Islam MT, Azim R and Mobashsher AT** (2012) Triple band-notched planar UWB antenna using parasitic strips. *Progress in Electromagnetics Research* **129**, 161–179.
15. **Tang M-C, Xiao S, Deng T, Wang D, Guan J, Wang B and Ge G-D** (2011) Compact UWB antenna with multiple band notches for WiMAX and WLAN. *IEEE Transactions on Antennas and Propagation* **59**, 1372–1376.
16. **Kim DO, Kim CY, Park JK and Jo NI** (2011) Compact band notched ultrawide band antenna using the Hilbert curve slot. *Microwave and Optical Technology Letters* **53**, 2642–2648.
17. **Ojaroudi M, Ghobadi C and Nourinia J** (2009) Small square monopole antenna with inverted T-shaped notch in the ground plane for UWB application. *IEEE Antennas and Wireless Propagation Letters* **8**, 728–731.
18. **Ojaroudi N, Ojaroudi M and Amir S** (2013) Compact UWB microstrip antenna with satellite down-link frequency rejection in X-band communications by etching an E-shaped step-impedance resonator slot. *Microwave and Optical Technology Letters* **55**, 922–926.
19. **Jahromi MN and Komjani N** (2008) Novel fractal monopole wideband antenna. *Journal of Electromagnetic Waves and Application* **22**, 195–205.
20. **Jahromi MN** (2008) Novel wideband planar fractal monopole antenna. *IEEE Transaction on Antennas and Propagation* **56**, 3844–3849.
21. **Cheema HM and Shamim A** (2013) The last barrier: on-chip antennas. *IEEE Microwave Magazine* **14**, 79–91.
22. **Bao XY, Guo YX and Xiong YZ** (2012) 60-GHz AMC-based circularly polarized on-chip antenna using standard 0.18-μm CMOS technology. *IEEE Transactions on Antennas and Propagation* **60**, 2234–2241.
23. **Pilard R, Gianesello F, Gloria D, Titz D, Ferrero F and Luxey C** (2011) 60 GHz HR SOI CMOS antenna for a System-on-Chip integration scheme targeting high data-rate kiosk applications. IEEE International Symposium on Antennas and Propagation (APSURSI), Spokane, WA.
24. **Yang W, Ma K, Yeo KS and Lim WM** (2012) A 60 GHz on-chip antenna in standard CMOS silicon Technology. IEEE Asia Pacific Conference on Circuits and Systems (APCCAS), Kaohsiung.
25. **Yan JB and Murch RD** (2007) Fabrication of a wideband antenna on a low-resistivity silicon substrate using a novel micromachining technique. *IEEE Antennas and Wireless Propagation Letters* **6**, 476–479.
26. **Jiang L, Mao JF and Leung KW** (2012) A CMOS UWB on-chip antenna with a MIM capacitor loading AMC. *IEEE Transactions on Electron Devices* **59**, 1757–1764.
27. **Kimoto K and Kikkawa T** (2005) Data transmission characteristics of integrated linear dipole antennas for UWB communication in Si ULSI. *IEEE Antennas and Propagation Society International Symposium* **1B**, 678–681.

28. **Karmakar A and Singh K** (2014) Planar monopole ultrawideband antenna on silicon with notched characteristics. *International Journal of Computer Applications*, ISSN 0975-8887, 17–20.
29. **Awasthi YK, Sharma M, Singh H, Kumar R and Kumari S** (2016) CPW-fed dual notched-band UWB antenna on silicon substrate. *International Journal of Innovative Research in Computer and Communication Engineering* **4**, 132–138.
30. **Chen ZN, See TSP and Qing X** (2007) Small printed ultrawideband antenna with reduced ground plane effect. *IEEE Transaction on Antennas and Propagation* **55**, 383–388.
31. **Abbosh AM and Bialkowski ME** (2008) Design of ultrawideband planar monopole antennas of circular and elliptical shape. *IEEE Transaction on Antennas and Propagation* **56**, 17–23.

Sanjukta Mandal received her B.Tech degree in Electronics & Instrumentation Engineering and M.Tech degree in Electronics & Communication Engineering from the University of Kalyani in 2012 and 2014, respectively. Her master's thesis was on frequency selective surface (FSS). She worked as a Project Fellow in the project entitled "Design of Mobile Robot Technology for Security, Surveillance, Mining, Building Inspection and Planetary Exploration (ESC0112/RP-1)" in CSIR-CMERI, Durgapur, West Bengal, India. She is currently pursuing her Ph.D. from the National Institute of Technology, Durgapur, West Bengal, India. Her current research interests include on-chip antenna design for short range communication and gain enhancement of on-chip antennas.

Ayan Karmakar received his B.Tech degree in Electronics and Communication from Maulana Abul Kalam Azad University of Technology, West Bengal (formerly known as WBUT) in 2005. Thereafter, he joined ISRO as a "Scientist" and subsequently posted to Semi-Conductor Laboratory (SCL), Chandigarh in Advanced Micro & Nano System Division. His research interests include design and development of L, S, C, X, and K-band passive microwave integrated circuits and antennas using silicon-based MIC and RF-MEMS technology. His fields of expertise are expanded in fabrication technology of various MEMS-based sensors and their testing strategies too. He completed his M.Tech from NIT-Durgapur with the specialization in Telecommunication. He serves as a reviewer for EJAET (*European Journal of Advanced Engineering and Technology*). He is the life member of IETE, India.

Harsh Vardhan Singh received his B.E. degree in Electronics & Communication Engineering from Rajiv Gandhi Proudyogiki Vishwavidyalaya, Bhopal in 2010. He received his M.Tech degree in Telecommunication Engineering from the National Institute of Technology Durgapur (NITD) in 2014. His master's work was on the reduction of SLLs and SBLs of time-modulated antenna arrays using various optimization algorithms. He is currently pursuing his Ph.D. degree at the NITD since 2015. His topic of research is the design of on-chip antennas for RF-telemetry applications. His research interest includes on-chip antennas, chip inductors, antenna arrays, and RF circuits for wireless communications.

Sujit Kumar Mandal received his B.Sc. degree in Physics Honours from the University of Calcutta in 2001. He completed his B.Tech and M.Tech in Radio Physics & Electronics from the Institute of Radio Physics & Electronics, C. U. in 2004 and 2006, respectively. He received his Ph.D. degree from the National Institute of Technology, Durgapur where he is presently working as an Assistant Professor in the Department of Electronics and Communication Engineering. His present research area includes application of soft computing techniques in antenna array optimization, time-modulated antenna arrays, microstrip patch antennas, RF-energy harvesting, and on-chip antenna design. Dr. Mandal is a member of IEEE.

Rajat Mahapatra was born in Kolkata, India in 1972. He received his M.Tech. and Ph.D. degrees from the Indian Institute of Technology (IIT) Kharagpur, India in 1999 and 2005, respectively. During 2005–2010, he was a Research Associate with the School of Electrical, Electronics and Communication Engineering, Newcastle University, Newcastle upon Tyne, UK. He is currently an Associate Professor with the Department of Electronics and Communication Engineering, National Institute of Technology (NIT), Durgapur, India. He has published about 80 articles in referred international journals and conference proceedings. His areas of interest include physics, technology and characterization of MOS devices, memory, and sensors.

Ashis Kumar Mal received his bachelors' degree in Electronics and (Tele)Communications Engineering from Bengal Engineering College (now IIEST) Shibpur and Masters' from IIT Kanpur in 1989 and 1994, respectively. He obtained his Ph.D. from IIT Kharagpur in 2009 in the field of Microelectronics and VLSI. He has about 25 years of teaching experience and currently with NIT Durgapur as an Associate Professor serving the Department of Electronics & Communication Engineering. He has published more than 60 articles in refereed international journals and conferences. He is an IEEE Solid-State Circuits Society (SSCS) member. His interest includes Analog/Mixed Signal VLSI (AMS) and digital-assisted analog (DAA).